The pressure dependences of elastic and lattice dynamic properties of AlAs from *ab initio* calculations*

Li Xing-Xiu(李兴秀)[a], Tao Xiao-Ma(陶小马)[a], Chen Hong-Mei(陈红梅)[a], Ouyang Yi-Fang(欧阳义芳)[a,b]†, and Du Yong(杜 勇)[b]

[a] *College of Physical Science and Technology, Guangxi University, Nanning* 530004, *China*
[b] *State Key Laboratory of Powder Metallurgy, Central South University, Changsha* 410083, *China*

(Received 13 May 2012; revised manuscript received 7 September 2012)

Ab initio calculations, based on norm-conserving nonlocal pseudopotentials and density functional theory (DFT), are performed to investigate the structural, elastic, dielectric, and vibrational properties of aluminum arsenide (AlAs) with a zinc-blende (B3) structure and a nickel arsenide ($B8_1$) structure under hydrostatic pressure. Firstly, the path for the phase transition from B3 to $B8_1$ is confirmed by analyzing the energies of different structures, which is in good agreement with previous theoretical results. Secondly, we find that the elastic constants, bulk modulus, static dielectric constants, and the optical phonon frequencies vary in a nearly linear manner under hydrostatic pressure. What is more, the softening mode of the transversal acoustic mode at the *X* point supports the phase transition in AlAs.

Keywords: mechanical properties, lattice dynamic properties, dielectric properties

PACS: 62.20.de, 63.20.D–, 77.22.–d **DOI:** 10.1088/1674-1056/22/2/026201

1. Introduction

Aluminum arsenide (AlAs) is one of the most promising III–V semiconductors with a zinc-blende structure (B3) in normal conditions. It exhibits excellent physical properties that make it attractive to device applications.[1] Technological interest in it has been stimulated in recent years by its potential applications in forming epitaxial multilayer structures with GaAs. It can be used in heterojunction bipolar transistors, Bragg reflector super lattices, solid state lasers, and high electronic mobility transistors.[2]

It is obvious that pressure is certainly a critical parameter for the structural stability, electronic and optical properties of a material. High pressure can yield a very large effect on the chemical and physical properties of materials, and can often exhibit new crystal phases with novel behaviors. Moreover, the possibility of studying structural stability as a function of pressure has added a new dimension to the fundamental question concerning the relation between atomic and electronic structure. With the development of the diamond anvil technique and the extension of the range for optical and X-ray measurements under static pressures, the pressure induced phase transition from B3 structure to the $B8_1$ structure in AlAs has been determined at a transition pressure of (7±5) GPa by Greene *et al*.[3] Meanwhile, using X-ray diffraction and electrical resistivity measurements, a phase transition pressure of 14.2 GPa was observed by Onodera *et al*.[4] In the theoretical field, the $B8_1$ phase of AlAs was postulated first by Froyen and Cohen[5] following the pseudopotential method in 1983. The qualitative high pressure behaviors of AlAs, such as structural properties,[6–15] band structure,[8–11,16–19] and dielectric properties,[9,20] were reported subsequently. But few people pay attention to the elastic properties and vibrational properties of AlAs under hydrostatic pressure. The elastic constant of a solid can give some interesting information about its mechanical and dynamical properties, and can provide a link between dynamical behavior and mechanical behavior of a material. Phonon excitation plays an important role in determining electronic transport, nonradioactive electron-relaxation processes, and other properties of interest for material characterization, device engineering, and design. Phonon dispersion is an interesting characteristic of a crystal. The optical and thermal properties can be revealed from the vibrational properties of a material. Therefore, the motivation of this work is to investigate the mechanical and vibrational properties under hydrostatic pressure using *ab initio* calculations.

The rest of the paper is organized as follows. In Section 2, the computational method is described. The calculated results are discussed and compared with the experimental and other theoretical data in Section 3. Finally, in Section 4, a brief summary is given.

2. Computational method

The calculations were performed using the plane-wave pseudopotential approach within the framework of the density-

*Project supported by the National Natural Science Foundation of China (Grant No. 11047031), the Natural Science Foundation of Guangxi Zhuang Autonomous Region, China (Grant No. 2011GXNSFC018003), and the Open Foundation of the Key Laboratory of New Processing Technology for Nonferrous Metals and Materials, China (Grant No. GXKFJ09-16).

†Corresponding author. E-mail: ouyanggroup@gmail.com

© 2013 Chinese Physical Society and IOP Publishing Ltd

functional theory (DFT) with CASTEP (Cambridge Serial Total Energy Package in Material Modeling, Accelrys).[21] The exchange–correlation energy of the electrons was described in the generalized gradient approximations (GGA) given by Perdew Burke Eenzerhof (PBE).[22] The valence electron–ion interaction was treated by *ab initio* norm-conserving pseudopotentials.[23] The aluminum $3s^2 3p^1$ electrons and arsenic $4s^2 4p^3$ electrons were treated as valence electrons. Well converged results were obtained using a kinetic energy cutoff of 816.0 eV and with a Monkhorst–Pack k-points mesh.[24] The total energy converged to better than 1 meV/atom. Phonon frequencies were calculated using the self-consistent density functional perturbation theory (DFPT),[25,26] which avoids the use of a supercell and allows calculation of the dynamical matrix at an arbitrary q vector. The DFPT also allows the calculation of the static dielectric tensor $\varepsilon(0)$ and the Born effective tensor charges Z_B for each inequivalent atom in unit cell. The phonon dispersion curves were calculated from the optimized geometry by employing the linear response method.[27,28] The elastic stiffness coefficient was determined using a finite strain technique[29] from a linear fitting of the computed stress based on adding small strains, where six strains amplitude up to a maximum of 0.3% were used.

3. Results and discussion

3.1. Structural properties and phase transformation

The equilibrium lattice constants are calculated by minimizing the total crystal energy obtained from different volumes and fitted to the Murnaghan's equation of state.[30] The calculated values of equilibrium lattice constants (a, c), bulk modulus (B_0), and first pressure derivative of bulk modulus (B_0') for AlAs with the B3 and $B8_1$ structures are all listed in Table 1 with available experimental data[3] and other theoretical results.[2,7,9,15,17] From Table 1, it can be seen that the values of the present calculated lattice constants, bulk modulus, and first pressure derivative of bulk modulus all agree well with the experimental data[3] and also with other theoretical results.[2,7,9,15,17]

The calculated energy–volume curves of an AlAs compound for the B3 and $B8_1$ structures are shown in Fig. 1. The inset shows the variations of enthalpy with pressure of B3 structure (solid line) and $B8_1$ structure (dashed line). It is clear that the pressure induced phase transition from the B3 structure to the $B8_1$ structure occurs at a transition pressure of 14.19 GPa, which is larger than other theoretical studies[2,7,9,13–15,17] as shown in Table 2. However, the present predicted transition pressure is in good agreement with the available experimental data with (7±5) GPa[3] and 14.2 GPa.[4] In order to gain an insight into the evolution of phase transition from B3 to $B8_1$ under pressure, the path of phase transition should be revealed. Figure 2 summarizes our findings and shows the path of the phase transition in a pressure–volume plot from B3 to $B8_1$ structure in AlAs. Firstly, the tetragonal angle γ of the B3 structure opens up from 90° to 120°, while the c/a ratio increases from $\sqrt{2}$ to $\sqrt{8/3}$. Then, the $B8_1$ phase occurs through the As atoms moving horizontally in the (001) plane. The path of the phase transition is in good agreement with the result of Cai[13] and Saitta.[31] According to Fig. 2, AlAs has a volume collapse of 18.8%.

Table 1. Calculated values of equilibrium lattice constants (a, c), bulk modulus (B_0), and first derivative of bulk modulus with pressure (B_0') for AlAs in B3 and $B8_1$ structures, and their comparison with other theoretical calculations and available experimental data.

Structure		a/Å	c/Å	B_0/GPa	B_0'
B3	This work	5.642	–	76.29	4.40
	Cal.[2]	5.637	–	75.2	4.39
	Cal.[7]	5.759	–	64.5	3.88
	Cal.[9]	5.632	–	76.66	3.808
	Cal.[15]	5.65	–	75.85	4.82
	Cal.[17]	5.72	–	76.41	4.16
	Exp.[3]	5.660	–	74±4	5.0±1
$B8_1$	This work	3.726	5.933	92.59	4.52
	Cal.[2]	3.724	5.911	93.3	4.58
	Cal.[7]	3.766	6.018	84.9	4.29
	Cal.[9]	3.722	5.878	91.987	4.203
	Cal.[17]	3.72	–	56.0	4.86
	Exp.[3]	3.790	6.054	73±7	4.6±0.7

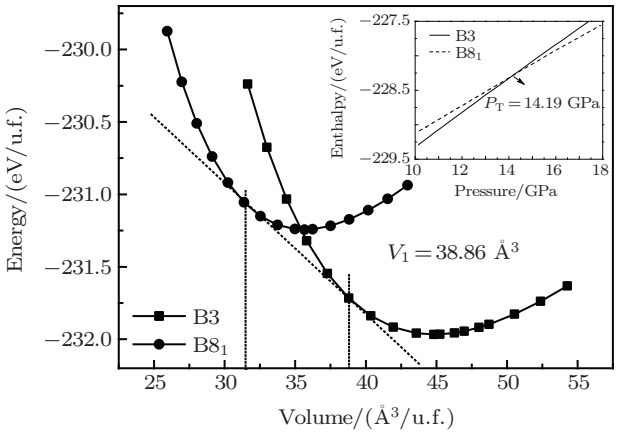


Fig. 1. Calculated energy–volume curves of AlAs. V_1 is the volume at the transition pressure. The inset shows the curves of enthalpy versus pressure.

Table 2. Calculated values of the phase transition pressure.

Phases	P_T/GPa		
	This work	Cal.	Exp.
B3→$B8_1$	14.19	6.1[2]	7±5[3]
		5.34[7]	14.2[4]
		6.68[9]	
		8.25[13]	
		10.5[14]	
		7.33[15]	
		6.99[17]	

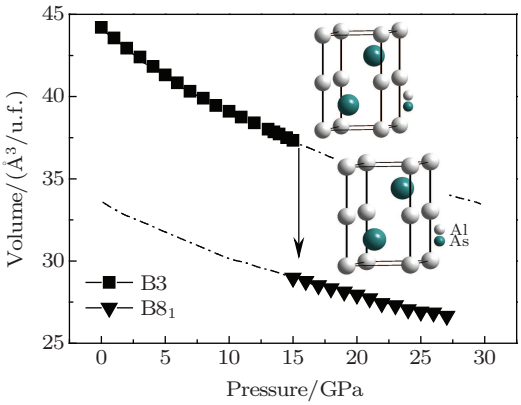


Fig. 2. (color online) Path of the phase transition from B3 to $B8_1$ structures for AlAs. The volume collapse at the transition pressure is 18.8%.

3.2. Elastic properties

The elastic constants for AlAs with B3 and $B8_1$ structures are listed in the following Table 3. From Table 3, the elastic constants of B3 structure are all in good agreement with the theoretical data.[8,16] To the best of our knowledge, no results on elastic constants for the $B8_1$ phase have been reported, that is, the present calculated elastic constants can be considered as predictions. The pressure dependences of the elastic constants of AlAs for both of the phases are shown in Fig. 3. It is clear that the value of C_{ij} increases linearly with pressure increasing.

Table 3. Elastic constants of AlAs in the B3 structure at zero pressure and in $B8_1$ structure at $P = 16.0$ GPa.

		C_{11}/GPa	C_{12}/GPa	C_{13}/GPa	C_{33}/GPa	C_{44}/GPa	C_{66}/GPa
B3	This work	119.2	54.8	–	–	60.4	–
	Cal.[8]	120.2	57.0	–	–	58.9	–
	Cal.[16]	116	55	–	–	57	
$B8_1$	This work	245.3	121.7	99.9	302.3	56.9	61.8

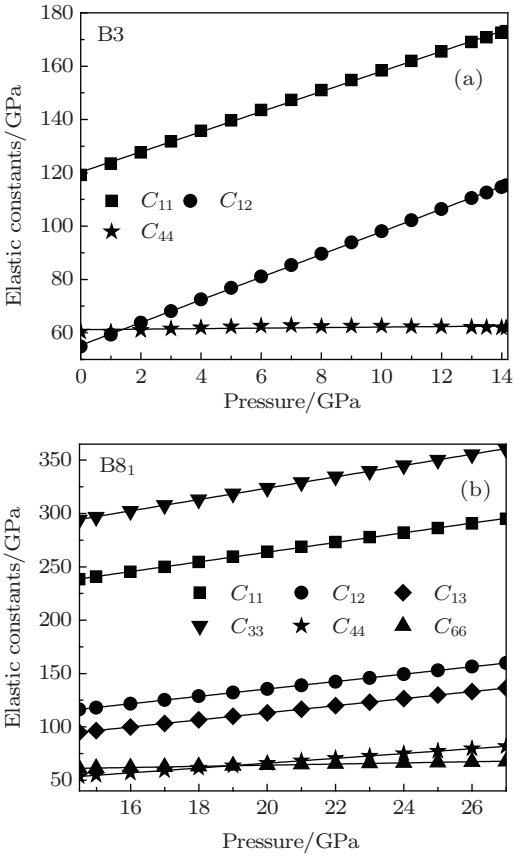


Fig. 3. Elastic constants (C_{ij}) of AlAs versus pressure in the B3 (a) and $B8_1$ (b) phases.

From the calculated results of single crystal elastic constants, bulk modulus (B), shear modulus (G), and Young's modulus (E) are determined using the Voigt–Reuss–Hill averaging scheme.[33–35] The pressure dependences of the bulk modulus (B) for both phases are shown in Fig. 4. It can be seen that bulk moduli of both phases increase linearly with pressure, and the value of bulk modulus in $B8_1$ structure is larger than that in B3 structure. The pressure dependences of shear modulus (G) and Young's modulus (E) are shown in Fig. 5. There is a hump peak in each of the curves of shear modulus (G) and Young's modulus (E) versus pressure before the phase transition for B3 phase. That means there is an energy peak of the distortion for the lattice structure during phase transition. In contrast, the shear modulus and Young's modulus for the $B8_1$ phase increase linearly with pressure.

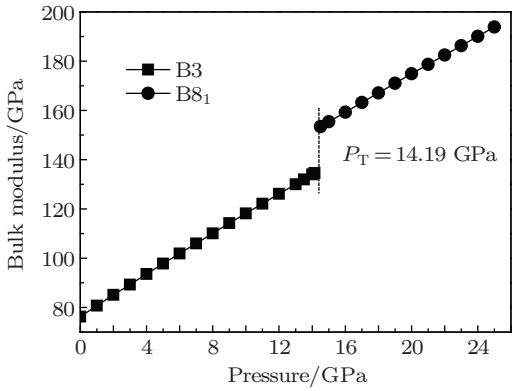


Fig. 4. Bulk modulus (B) of AlAs versus pressure in the B3 and $B8_1$ phases.

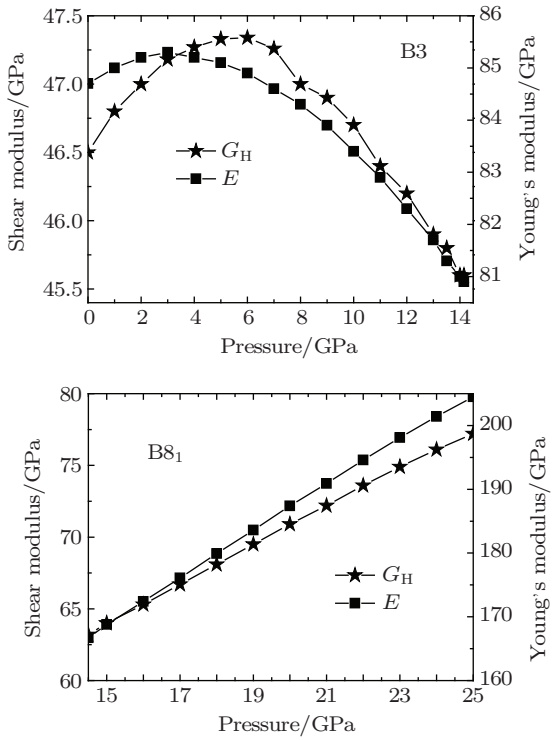


Fig. 5. Curves of shear modulus (G) and Young's modulus (E) of AlAs versus pressure in the B3 and $B8_1$ phases.

3.3. Dielectric properties

Since the B3–AlAs has cubic symmetry, only one dielectric tensor component can completely characterize the linear optical properties. This component is $\varepsilon_2(\omega)$, the imaginary part of the frequency-dependent dielectric function is expressed as[36]

$$\varepsilon_2(\omega) = \frac{1}{\pi}\left[\frac{e}{m\omega}\right]^2 \sum_{ij} \int_{\mathrm{BZ}} f_{ij} P_{ji} P_{ij} \delta(E_{ji} - \hbar\omega)\,\mathrm{d}k, \qquad (1)$$

where m is the mass, ω is the frequency, k is the wave vector, $E = \hbar\omega$, $E_{ji} = E_j - E_i$, and $f_{ij} = f_i - f_j$, with f_i being the Fermi occupation factor of the single-particle state i, P_{ij} is the momentum matrix element. The subscripts i and j indicate the conduction and valence band, respectively. It should be noted that the BZ stands for Brillouin zone.

The imaginary parts of the dielectric function of B3–AlAs at $P = 0.0$ GPa and $P = 12.0$ GPa are shown in Fig. 6. The pressure makes both the shape and the position of the main peaks of the $\varepsilon_2(\omega)$ vary successively, which accords well with the previous first-principles studies.[9] The curve of calculated energy of the main peak of $\varepsilon_2(\omega)$ versus pressure is shown in Fig. 7. The calculated energy of the main peak varies almost linearly as pressure increases.

To deal with the macroscopic electric field associated with the longitudinal optical mode and the relevant non-analytic behavior of the dynamical matrix at Γ point, we calculate static dielectric constant ε_0 and Born effective charge Z_B tensors for AlAs in the B3 structure, which are isotropic scalars in cubic symmetry. The Born effective charge is a fundamental quantity that specifies the leading coupling between lattice displacement and electrostatic field in insulator. The pressure dependence of Born effective charge Z_B and static dielectric constant ε_0 for the B3 phase are shown in Fig. 8. The Born effective charge Z_B decreases linearly with pressure increasing, while the static dielectric constant decreases quadratically with the increase of pressure.

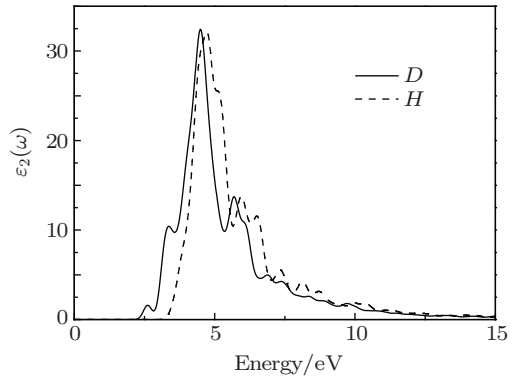


Fig. 6. Imaginary parts of the dielectric function of AlAs in the B3 phase at $P = 0$ GPa and $P = 12.0$ GPa.

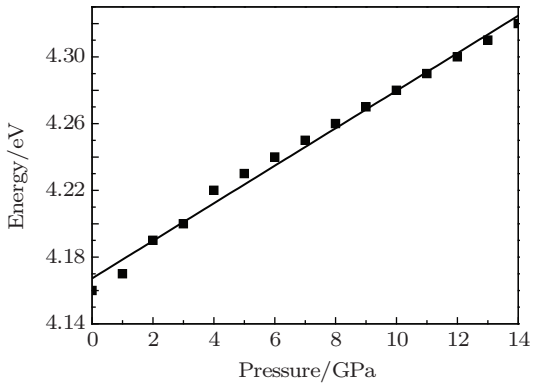


Fig. 7. Calculated energy of the main peak of $\varepsilon_2(\omega)$ versus pressure for B3 AlAs.

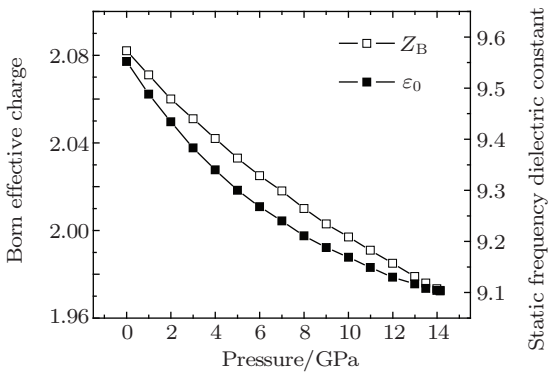


Fig. 8. Born effective charge and static dielectric constant of AlAs versus pressure in the B3 phase.

3.4. Vibrational properties

The phonon spectra of B3–AlAs and $B8_1$–AlAs are calculated. The calculated values of the phonon frequency ω_i, pressure derivative of the phonon frequencies, and mode Grüneisen parameter γ_i at Γ point for B3–AlAs and $B8_1$–AlAs at zero pressure and at $P = 16.0$ GPa are listed in Table 4. For B3–AlAs, $\omega_{LO}(\Gamma) = 399.1$ cm^{-1} and $\omega_{TO}(\Gamma) = 363.8$ cm^{-1}, respectively, for transverse optical phonon (TO) mode and longitudinal optical phonon (LO) mode zone central phonons accord well with experimental values ($\omega_{LO}(\Gamma) = 399.59$ cm^{-1} and $\omega_{TO}(\Gamma) = 360.04$ cm^{-1}) reported by Lockwood *et al.*[37] To the best of our knowledge, there are no experimental data or theoretical results available for AlAs in the $B8_1$ structure. At Γ point for AlAs in the $B8_1$ structure, there are three acoustic and nine optical phonon modes: E_{2u}, E_{2g}, A_{2u}, B_{1g}, E_{1u}, and B_{2u}, where E_{2g} mode is Raman-active. What is more, the optical phonon frequencies of B3 and $B8_1$ structures increase linearly with pressure increasing.

Table 4. Values of phonon frequency ω_i, mode Grüneisen paramater γ_i, first and second derivative of the frequency at Γ point with respect to pressure, obtained for AlAs in B3 and $B8_1$ structures, respectively, at $P = 0$ GPa and $P = 16.0$ GPa.

Structure	Mode	ω_i	γ_i/(cm^{-1}/Å^3)	$(\partial\omega/\partial P)$/(cm^{-1}/GPa)	$(\partial^2\omega/\partial P^2)$/(cm^{-1}/GPa^2)
B3	TO	363.8	1.26	5.90	–0.09
	LO	399.1	1.11	5.69	–0.10
$B8_1$	E_{2g}	201.3	1.40	1.77	–0.03
	E_{2u}	228.9	2.56	3.68	–0.07
	B_{2g}	234.4	1.48	2.18	–0.04
	E_{1u}	318.0	2.01	4.02	–0.07
	A_{2u}	335.2	1.91	4.03	–0.06
	B_{1u}	462.5	1.15	3.34	–0.06

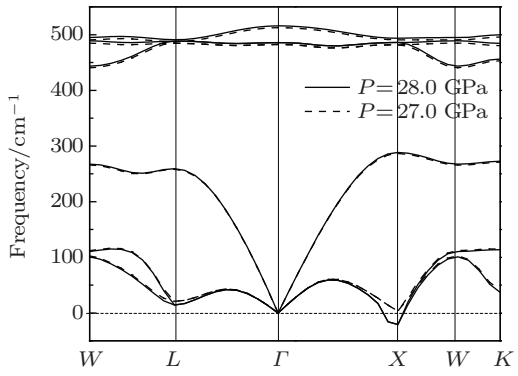


Fig. 9. Phonon dispersion curves of AlAs in the B3 phase at $P =$ 27.0 GPa and 28.0 GPa.

The calculated phonon dispersion curves of AlAs in B3 structure at $P = 27.0$ GPa and 28.0 GPa are shown in Fig. 9. Comparison between the curves of $P = 27.0$ GPa and those of $P = 28.0$ GPa clearly shows that the transversal acoustic modes at X point obtain softening modes at $P = 28.0$ GPa. In other words, the B3 structure is unstable at $P = 28.0$ GPa for AlAs, which would be changed into the other structure. The phase transition pressure ($P_T = 27.0$ GPa) from phonon mode softening is much larger than the value of calculated equal enthalpies of the two phases ($P_T = 14.19$ GPa), because the transformation from B3 phase to $B8_1$ phase for AlAs must overcome a potential barrier, which is caused by the hysteresis in the atoms moving and is much higher than the transition pressure.

4. Summary

In summary, *ab initio* calculations are adopted to investigate the structural, elastic, dielectric, and vibrational properties of AlAs with zinc-blende (B3) and nickel arsenide ($B8_1$) phases under hydrostatic pressure. The calculated values of lattice, bulk modulus, and elastic constants are all in good agreement with experimental data and other first principles calculations. We find that elastic constants, Bulk modulus, static dielectric constants, and optical phonon frequencies vary almost linearly hydrostatic pressure. However, Born effective charges decrease with pressure increasing quadratically. For the characterization of phase transition, the phonon dispersion curves in the B3 phase are investigated. We hope that our work will stimulate future high-pressure Raman and X-ray experiments in AlAs.

References

[1] Kimukin I, Biyikli N, Kartaloglu T, Aytur O and Ozbay E 2004 *IEEE J. Selected Top. Quantum Electron.* **10** 766
[2] Liu G C, Lu Z W and Klein B M 1994 *Phys. Rev.* B **51** 5678
[3] Greene R G, Luo H, Li T and Ruoff A L 1994 *Phys. Rev. Lett.* **72** 2045
[4] Onodera A, Mimasaka M, Sakamoto I, Okumura J, Sakamoto K, Uehara S, Takemura K, Shimomura O, Ohtani T and Fujii Y 1999 *J. Phys. Chem. Solids* **60** 167
[5] Froyen S and Cohen M L 1983 *Phys. Rev.* B **28** 3258
[6] Adachi S 1987 *J. Appl. Phys.* **61** 4869
[7] Wang H Y, Li X S, Li C Y and Wang K F 2009 *Mater. Chem. Phys.* **117** 373
[8] Adachi S 1985 *J. Appl. Phys.* **58** 3
[9] Amrani B 2006 *Sup. Micro.* **40** 65
[10] Aourag H, Ferhat M, Bouhafs B, Bouarissa N, Zaoui A, Amrane N and Khelifa B 1995 *Comput. Mater. Sci.* **3** 393

[11] Aouina NY, Mezrag F, Boucenna M, Farra ME and Bouarissa N 2005 *Mater. Sci. Eng.* B **123** 87
[12] Annane F, Meradji H, Ghemid S and Hassan FEH 2010 *Comput. Mater. Sci.* **50** 274
[13] Cai J and Chen N X 2007 *Phys. Rev.* B **75** 174116
[14] Singh R K and Singh S 1992 *Phys. Rev.* B **45** 1019
[15] Gupta D C and Kulshrestha S 2009 *Phase Transitions* **82** 850
[16] Chetty N, Muñoz A and Martin R M 1989 *Phys. Rev.* B **40** 11934
[17] Srivastava A, Tyagi N, Sharma U S and Singh R K 2011 *Mater. Chem. Phys.* **125** 66
[18] Wei S H, Nie X, Batyrev I G and Zhang S B 2003 *Phys. Rev.* B **67** 165209
[19] Godby R W 1988 *Phys. Rev.* B **37** 10159
[20] Reshaka A H and Auluck S 2007 *Physica* B **395** 143
[21] Segall M D, Lindan P J D, Probert M J, Pickard C J, Hasnip P J, Clark S J and Payne M C 2002 *J. Phys.: Condens. Matter* **14** 2717
[22] Perdew J P, Burke K and Ernzerhof M 1996 *Phys. Rev. Lett.* **77** 3865
[23] Lin J S, Qteish A, Payne M C and Heine V 1993 *Phys. Rev.* B **47** 4174
[24] Monkhorst H J and Pack J D 1976 *Phys. Rev.* B **13** 5188
[25] Baroni S, Giannonzzi P and Testa A 1987 *Phys. Rev. Lett.* **58** 1861
[26] Giannozzi P, Gironcoli S, Pavone P and Baroni S 1991 *Phys. Rev.* B **43** 7231
[27] Gonze X, Allan D C and Teter M P 1994 *Phys. Rev. Lett.* **68** 3603
[28] Gonze X 1997 *Phys. Rev.* B **55** 10337
[29] *CASTEP Users Guide* (San Diego: Accelrys Inc., CA, 2005) and references therein
[30] Murnaghan F D 1944 *Proc. Natl. Acad. Sci. USA* **50** 697
[31] Saitta A M and Decremps F 2004 *Phys. Rev.* B **70** 035214
[32] Aouadi S, Hernandez P R, Kassali K and Muñoz A 2008 *Phys. Lett.* A **372** 5340
[33] Voigt W 1928 *Lehrbuch der Kristallphysik, Taubner*, Leipzig
[34] Reuss A and Angew Z 1929 *Math. Mech.* **9** 55
[35] Hill R 1952 *Proc. Phys. Soc. London* Sect. A **65** 350
[36] Moss D J, Ghahramani E, Sipe J E and van Driel H M 1990 *Phys. Rev.* B **41** 1542
[37] Lockwood D J, Yu G L and Rowell N L 2005 *Solid State Commun.* **136** 404